Proceedings of the 16th International Conference on Soil Mechanics and Geotechnical Engineering

doi:10.3233/978-1-61499-656-9-2631

Large-diameter cyclic triaxial tests for seismic safety assessment of an earth dam

Essais triaxiaux cycliques en gros diamètre pour évaluer la sécurité sismique d'un barrage en terre

R.P. Brenner, M. Wieland & S. Malla
Electrowatt-Ekono Ltd., CH-8037 Zurich, Switzerland

ABSTRACT

Large-diameter (300 mm) cyclic triaxial tests were conducted on morainic, non-plastic soil taken from the core of the 117 m high Mattmark dam in Switzerland with the objective to provide an estimate of excess pore pressure development and the deformations under cyclic loading caused by the strongest possible earthquake in that region. Variables considered were anisotropic consolidation stresses, cyclic stress amplitude and number of cycles as derived from a dynamic response analysis of the dam. The results indicated that the build up of excess pore pressures remained small but the deformations produced by cyclic loading could be substantial, i.e. exceeding 5 %. Analysis of seismic settlement, however, showed that the safety of the dam is not compromised.

RÉSUMÉ

On a réalisé des essais triaxiaux cycliques en gros diamètre (300 mm) sur des sols morainiques prélevés du noyau du barrage de Mattmark en Suisse. Le but de ces essais était d'obtenir une estimation des pressions interstitielles et des déformations générées par les sollicitations cycliques causées par le séisme maximum pour cette région. Les variables considérées étaient les contraintes de consolidation anisotropique, le taux de cisaillement dynamique et le nombre de cycles obtenues de l'analyse dynamique du barrage. Les résultats montrent que le développement des pressions interstitielles reste faible mais que les déformations due aux sollicitations cycliques peuvent être importantes, c'est-à-dire supérieures à 5%. L'analyse des tassements sismiques montre que la sécurité du barrage n'était pas compromise.

1 INTRODUCTION

Mattmark dam, constructed in the 1960s, is a 117 m high zoned earthfill embankment. It forms part of a hydro-electric scheme in the southern part of Switzerland (Fig. 1). For a planned increase in the reservoir level by 2 m, the Swiss Federal Office of Water and Geology (BWG) required an assessment of the seismic safety of the dam according to the new BWG guideline established in the year 2000, to ensure that deformations remained within tolerable limits and would not lead to insufficient freeboard or internal erosion along weak zones or shear surfaces.

The investigations carried out involved both laboratory testing of dam materials and numerical analysis evaluating the response of the dam under seismic loading caused by an earthquake with a return period of 10,000 years. Details of the dynamic analysis and results were presented by Wieland and Malla (2002). This paper summarizes the experience gained with cyclic triaxial tests, which were an important part of the laboratory testing program, and discusses the relevance of the results to dam safety.

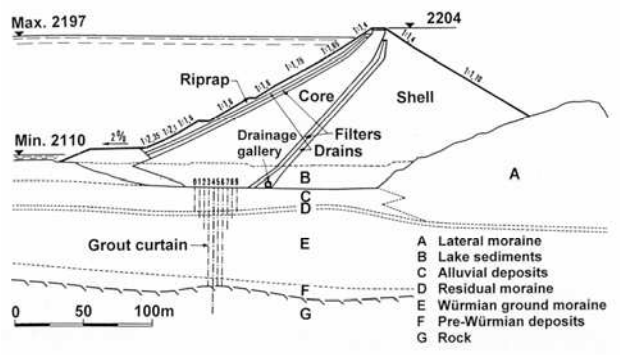

Figure 1. Typical section of Mattmark dam

Mattmark dam is built entirely of non-plastic materials derived from two lateral moraines (glacial till) located in the vicinity of the site, namely the Allalin and the Schwarzberg moraines. The core material was produced by processing the morainic soil through a wobbler which removed most of the particles larger than 100 mm. Figure 2 shows the grain size distribution curves of the various material zones obtained during the construction period and Table 1 lists material parameters determined during the design stage and also during construction. Detailed information on material properties and the construction of the embankment was given by Gilg (1974).

Table 1: Material characteristics

Material zone	φ' (°)	c' (kPa)	ρ_d (Mg/m^3)	ρ_s (Mg/m^3)	k (m/s)
Core	42.0	0.20	2.48	2.99	1-2x10^{-7}
Filter	39.7	0.80	2.20	2.82	3x10^{-6}
Drainage	38.7	0.75	2.04	2.82	2x10^{-3}
Shell	42.6	0	2.45	2.99	>10^{-3}
Foundation	34.2	0.40	2.14	2.78	variable

ρ_d=dry density, ρ_s=grain density, k=hydraulic conductivity

2 PROGRAM FOR CYCLIC TRIAXIAL TESTS

2.1 *Sampling*

Samples, about 0.6 m^3 each, were taken from backhoe-excavated pits on the dam crest at two locations (Materials 1 and 2a). Sampling depth was between 2.20 and 2.70 m. Another sampling location was downstream of the dam in a former borrow area at the Allalin moraine (Material 3).

Materials 1 and 2a are basically identical; they originate from the Schwarzberg moraine and represent the core material.

All tests in this program were carried out at two laboratories equipped with large-size testing facilities.

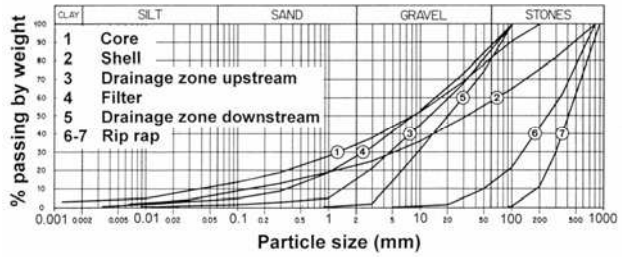

Figure 2. Average grain size distribution curves of dam materials

2.2 *Isotropically consolidated drained triaxial tests*

For reference and to verify previous results obtained during the construction period, three drained multistage triaxial tests were carried out on Materials 2a, 2b and 3. Material 2a was labeled 2b after dislocation of the material to the LMSSM laboratory because it showed a different behavior in that its grain size distribution had practically no fines, probably as a result of segregation during storage and transport.

Consolidation pressures for the multistage tests were 50, 100 and 150 kPa with a back pressure of 400 kPa. The rate of shearing was determined by carrying out one test with pore water pressure measurement. In the third stage shearing was continued until an axial strain of 10 % was reached.

The test specimens had a diameter of 300 mm and a height of 600 mm. The material, scalped at 50 mm, was compacted inside the rubber membrane at a water content corresponding more or less to the field value during construction, i.e. at around 5 to 6 %. The target densities to reach were 2.40 Mg/m^3 for the material obtained from the Allalin moraine (Material 3) and 2.20 to 2.26 Mg/m^3 for that from the Schwarzberg moraine (Material 2b).

2.3 *Consolidated undrained cyclic triaxial tests*

There were altogether eleven tests on Materials 2b and 3. All samples were prepared in the same way with the following targets: ρ_d = 2.30 Mg/m^3, water content w = 5.5 % for material 2b and ρ_d = 2.40 Mg/m^3, w = 6.0 % for Material 3. All test conditions are listed in Table 2. Test variables were the effective confining pressure, σ_{3c}', the anisotropy ratio, $\sigma_{1c}'/\sigma_{3c}'$, the cyclic stress amplitude, the rate of loading during the first cycle, and the frequency.

Table 2: Program of cyclic triaxial tests

Test no	σ_{1c}' (kPa)	σ_{3c}' (kPa)	e_c	$(\sigma_1-\sigma_3)_{max}$ (kPa)	$(\sigma_1-\sigma_3)_{min}$ (kPa)	N
Material 3						
1	285	67	0.167	400	90	-
2	285	67	0.171	275	138	50
3	285	67	0.173	600	62	50
4	199	69	0.155	310	50	50
7	300	100	0.167	282	12	50
10	285	67	0.206	430	65	3
11	285	67	0.200	349	103	34
Material 2b						
5	285	67	0.232	133	-	0
6	200	67	0.160	208	50	13
8	200	70	0.239	172	107	50
9	200	70	0.218	261	45	13

N= number of cycles; e_c=void ratio after anisotropic consolidation
Tests 1,2 and 3: 1st cycle slow

The initial stress conditions (consolidation under σ_{1c}', σ_{2c}' = σ_{3c}') were obtained from a 2-D finite element analysis using an elasto-plastic material model (Mohr-Coulomb) and pore water pressures resulting from a flow net for steady-state flow (for details see Wieland and Malla, 2002). Saturation of the samples was ensured by a back pressure of 800 kPa, checked by Skempton's B parameter (B = $\Delta u/\Delta\sigma_3$). Consolidation was first under isotropic stresses (σ_{1c} = σ_{3c}) at 850 kPa. This phase was terminated when the pore pressure in the center of the specimen had reached the value of the back pressure. Subsequently, further consolidation under an anisotropic stress state occurred by increasing the axial stress.

After having reached zero excess pore water pressure under the anisotropic stress state, the samples were subjected to cyclic undrained loading by varying the axial stress. The radial stress was kept constant. During the test, the pore water pressure at the center of the sample, the axial deformation, the applied force and the volume change were monitored continuously.

The cyclic stress amplitude was determined by a 2-D finite element (FE) dynamic response analysis, which yielded the cyclic shear stress on the horizontal plane of each element. For this analysis the variations of shear modulus and damping with shear strain were derived from degradation curves given by Seed et al. (1984). Figure 3 shows the FE mesh and the shear stress history of element 198.

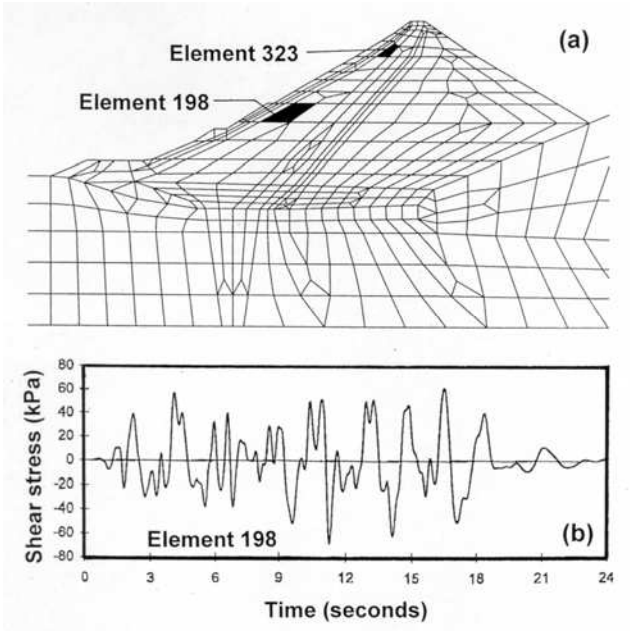

Figure 3. Dynamic response analysis: (a) Finite element model; (b) horizontal shear stress history of element 198

The dynamic loading of the soil in situ was then modeled by applying a stress history consisting of a number of cycles with constant shear stress amplitude, τ_d=0.65$\tau_{d\,max}$, to selected elements. These element were those where the ratio $\tau_{d\,max}/\sigma_z'$ was large (σ_z' is the vertical effective stress at the location of the element considered). The elements studied were 198 and 323. There were some elements that reached yield conditions already under static loading. These were located at the upstream base of the core. The modeling of these elements under additional cycles of loading was not feasible because strains would be too large and the capacity of the equipment would be exceeded. The static stresses calculated for elements 198 and 323 are listed in Table 3.

Table 3 Stresses in elements 198 and 323

Element	Static stresses					$\tau_{d\ max}$	τ_d
	σ_1'	σ_3'	σ_x'	σ_z'	$\tau_{xz\ stat}$		
198	285	67	114	240	90	60	39
323	199	69	101	167	56	35	23

$\tau_d = 0.65\ \tau_{d\ max}$

The horizontal plane of an element is loaded by the vertical stress, σ_z' and the static shear stress, $\tau_{xz\ stat}$. The superposition of a dynamic stress, τ_d, on this horizontal plane is simulated by an increase or decrease of the major principal stress, σ_1, while σ_3 is kept constant.

The number of cycles was limited to 50. The pore pressure was measured at the top and at the center of the specimen, by a needle, 10 cm long, placed at mid-height of the specimen. The frequency was generally kept at 0.1 Hz, however, initially some tests were conducted with their first cycle at 0.01 Hz.

3 TEST RESULTS

3.1 *Grain size distribution*

Originally, the three samples (Materials 1, 2a, and 3) had nearly identical grain size distributions. They followed the fine-grained boundary of the range established for the core material during construction. Figure 4 shows the grain size distribution of the materials tested together with the range obtained during construction, scalped at 50 mm. Material 2b is usually coarser and falls in between the ranges that were given for filter and drains (not shown in Fig. 4).

3.2 *Static triaxial tests*

Table 4 lists the results obtained from the three multistage tests (w_i = initial water content)

Table 4 Results from multistage static triaxial tests

Material	w_i (%)	ρ_d (Mg/m^3)	c' (kPa)	φ' (^{o})	φ_c' (^{o})	K	n
2a	5.7	2.28	10	45	43	720	0.8
3	6.2	2.46	10	45	41	720	0.8
2b	5.5	2.32	0	40	38	410	0.8

These values are comparable to those obtained during construction (see Table 1) but the cohesion is smaller.

The critical state of the material, defined as the condition when plastic shearing can continue without changes in volume or effective stress, is expressed in the Mohr-Coulomb diagram by a straight line, the critical state line (CSL), passing through the origin with a slope tan φ_c'.

The results also permit the estimation of Poisson's ratio, ν, measured in the initial phase of contraction, i.e. for axial strains $\varepsilon_1 < 1\%$. The value for all three materials is 0.36.

The drained secant modulus at $\varepsilon_1 = 5x10^{-3}$ is a function of the isotropic consolidation pressure, σ_{3c}'. Similar values were found for Materials 2a and 3 but the value was lower for Material 2b. The deformation modulus can be expressed as a function of the mean effective consolidation pressure, σ_m', namely:

$$E_{0.5\%} = K\ p_a\ (\sigma_m'/p_a)^n$$

where: $\sigma_m' = (\sigma_1'+2\sigma_3')/3$, p_a = atmospheric pressure, K= non-dimensional parameter, and n = exponent. The value of 0.8 for n corresponds to other morainic soils from the alpine region. Values for K and n are also shown in Table 4.

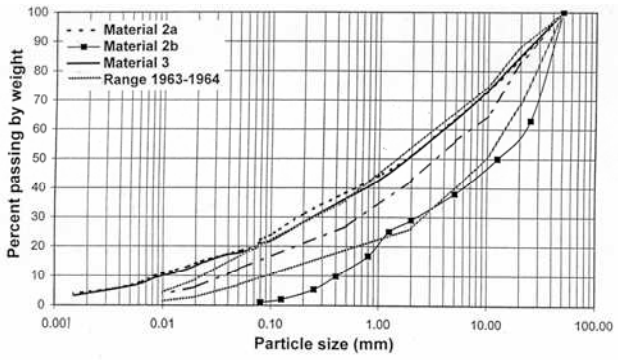

Figure 4. Grain size distribution curves of materials tested (2a, 2b, and 3) and of materials used during construction

3.3 *Cyclic triaxial tests*

3.3.1 *Material 3*

Of interest for the safety evaluation of the dam are the stress paths, the axial deformations, and the pore water pressures.

The stress path followed during anisotropic consolidation and cyclic loading is shown in Fig. 5a for Test 7. The following features can be seen: (1) The point representing the end of anisotropic consolidation is located distinctly below the CSL (c'=0 and φ_c'=41°) for tests with low K_c (e.g. $K_c=\sigma_1'/\sigma_3'$=3.0 in Test 7); this point moves closer to the CSL for a higher anisotropy ratio (not shown in Fig. 5); and (2) after the first cycle, which is strongly dilatant, the stress path stabilizes and becomes tangential to the critical state line without crossing it.

The axial deformation at the end of cyclic loading depends on the density (or void ratio) of the sample and on the maximum deviator stress. For example, in Fig. 6, Tests 10 and 11 with higher void ratios show larger deformations than Tests 1 and 2. In Tests 3, 10, and 11 the central part of the specimen came into contact with the cell wall. Hence, interpretation of these results

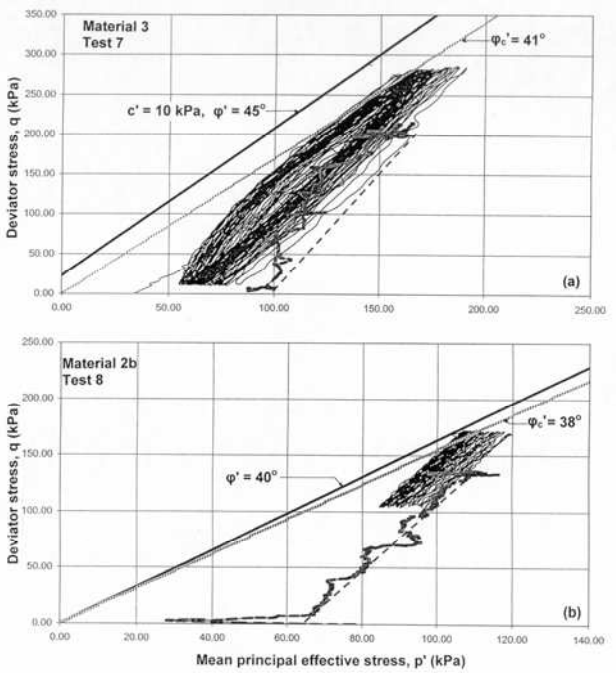

Figure 5. Anisotropic consolidation followed by cyclic loading at 0.1 Hz: (a) Material 3, Test 7; (b) Material 2b, Test 8

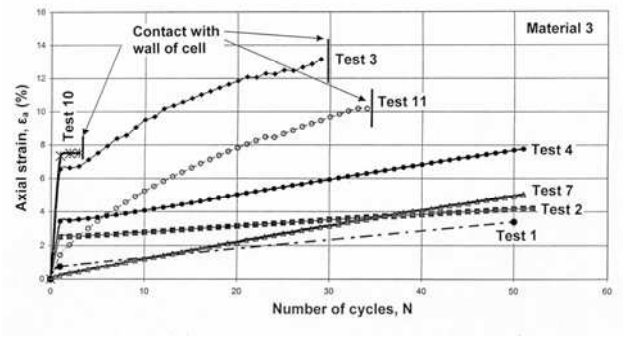

Figure 6. Axial deformation at end of N cycles: Material 3, Tests 1, 2, 3, 4, 7, 10, and 11

is limited to the part before contact occurred. For example, in Test 10 only three cycles were possible.

The residual axial deformations generated by the cyclic loading are less than 5 % in 15 cycles (which is the equivalent number of cycles of an earthquake of magnitude 7.5) for all tests except Tests 3, 10, and 11 where the stresses are large with respect to the density of the specimens. These tests also had the highest cyclic stress amplitudes.

Figure 7 shows the development of pore water pressures at the center of the specimen at the end of each cycle as a function of the number of cycles in a semi-log scale for all tests except Test 1. The dilatant character of the material is reflected by the development of negative pore water pressures during the first cycle loading. The high back pressure prevents cavitation. At the end of the 1st cycle, the pore water pressure can be significantly negative (-60 to –80 kPa), slightly negative (-5 to –10 kPa) or even slightly positive. However, as can be seen, the pore water pressure development in three tests where 50 cycles did not cause a contact with the cell wall, is small. It always remained below 20 kPa at the end of 50 cycles.

3.3.2 *Material 2b (Tests 5, 6, 8, and 10)*

Figure 5b shows the stress path of Test 8. The point representing the end of anisotropic consolidation is located clearly below the CSL (c'=0, φ_c'=38°). Under low cyclic stresses, the cycles stay below the CSL, even after 50 cycles.

Regarding axial deformations, only Test 8 was amenable to interpretation. The other tests suffered deformations from the beginning of the test and came into contact with the wall of the cell. Material 2b turned out to be much more deformable with the number of cycles than Material 3. Also Material 2b was dilatant in all the tests during the first cycle loading and pore water pressure development followed a pattern similar to that of Material 3.

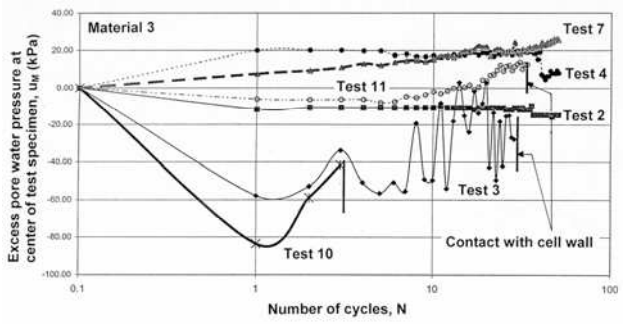

Figure 7. Pore water pressure response during cyclic loading: Material 3, Tests 2, 3, 4, 7, 10, and 11

4 APPLICATIONS TO SAFETY OF MATTMARK DAM

Test results relevant to dam safety after raising of the reservoir level are those affecting stability of the dam body and deformation of the crest. Possible scenarios to occur during a strong earthquake are excess pore water pressure build up and reduction of the shear strength to residual values caused by cyclic loading.

The permeability of the core material, estimated at about $2x10^{-7}$ m/s for Material 3, is considered small enough to assume perfectly undrained behavior during earthquake loading, even for layers close to the drains. The dilatant character of the core material during shearing limits the generation of significant excess pore water pressures, as illustrated in Fig. 7. A liquefaction scenario can therefore be excluded.

The tests have shown that residual deformations at the end of cyclic loading can reach substantial values, i.e. in excess of 5 %. The deformations depend on the initial density (or void ratio), the initial stress state (particularly the shear stress on a horizontal plane at any point) and the cyclic stress amplitude. A high anisotropy ratio together with a high initial shear stress on the horizontal plane produces large deformations also in dense soils. For example, Test 3 with $\tau_{d\ max}$=120 kPa results in large deformations in spite of a low void ratio.

The total deformation at the dam crest is the sum of the settlement due to dynamic loading and the vertical displacement caused by the potential sliding of soil bodies in the crest region. The latter can be estimated from a Newmark type sliding block analysis using residual strength values along the sliding surfaces. Wieland and Malla (2002) found that the total vertical displacement at the crest would not exceed 1.5 m, which is acceptable in view of the freeboard requirements.

5 CONCLUSIONS

The cyclic triaxial laboratory tests on two types of soils representing essentially the core and filter material of Mattmark dam have demonstrated that:

(1) The generation of excess pore water pressures during cyclic loading after 50 cycles is not significant because the soils tested behaved dilatant.

(2) The residual deformations at the end of cyclic loading can be substantial, i.e. 5% or more. However, potential sliding bodies in the crest region do not compromise the freeboard requirements.

(3) The reservoir level can be raised by 2m fully satisfying the safety requirements of the BWG guidelines.

ACKNOWLEDGEMENT

The large-diameter cyclic triaxial tests were carried out by Geodynamique et Structure in France.

REFERENCES

Gilg, B. 1974. Mattmark - a dam founded on alluvial and morainic deposits. *Proc. Eng. Found. Conf. on Foundations for Dam*, Pacific Grove, CA, American Society of Civil Engineers, pp.215-248.

Seed, H.B., Wong, R.T., Idriss, I.M. and Tokimatsu, K. 1984. *Moduli and damping factors for dynamic analysis of cohesionless soils*. Report No. UCB/EERC-84-14, Earthquake Eng. Research Center, Univ. of Calif.

Wieland, M. and Malla, S. 2002. Seismic evaluation of a 117 m high embankment dam resting on a thick soil layer. *Proc. 12th European Conf. on Earthquake Engineering*, London, UK, Paper 128.